Critical and Spin-Wave Fluctuations in Nickel by Neutron Scattering*

V. J. MINKIEWICZ,† M. F. COLLINS,‡ R. NATHANS,§ AND G. SHIRANE
Brookhaven National Laboratory, Upton, New York 11973
(Received 9 December 1968)

This paper gives direct measurements of the frequency- and wave-vector-dependent critical scattering of neutrons from nickel. Extensive measurements have been made around the Curie temperature to study the critical fluctuations in detail, particular emphasis being placed on the dynamics of these fluctuations. Below the Curie temperature T_c, the fluctuations can be described in terms of spin-wave excitations with an exchange stiffness constant D that varies with temperature as $(1-T/T_c)$ to the power 0.39 ± 0.04. The spin waves become over-critically damped just below T_c. Right at the critical temperature, the energy width of the scattering is observed to vary as the wave vector q to the power 2.46 ± 0.25, in excellent agreement with the predictions of the dynamic scaling laws. Above T_c, in the hydrodynamic region, the spin-diffusion constant is observed to vary as $(1-T_c/T)$ to the power 0.51 ± 0.05, in marked contrast to theoretical predictions of a value close to 0.33. Comparison with our recent data for iron suggests that spin diffusion in the two materials may be occurring with different dominant mechanisms. As in iron, no scattering was observed from diffusive components of the susceptibility for $T<T_c$; this result contrasts strongly with the scattering observed from the Heisenberg antiferromagnet $RbMnF_3$, where a diffusive mode is clearly seen. Extensive data have been taken of the spin-wave dispersion relations at room temperature. Interpretation of the data in terms of a Heisenberg model leads to the conclusion that the exchange is long-range in extent, with ferromagnetic interactions present over short ranges and antiferromagnetic interactions predominating over longer ranges.

I. INTRODUCTION

THE magnetic scattering of thermal neutrons is a technique of unique value for establishing both the static and the dynamic properties of magnetic correlations. It has already been extensively applied to the study of the static magnetic properties of the 3*d* metals. However, only with the advent of more intense slow neutron sources and recent developments in the experimental technique, has it become possible to measure the long-wavelength inelastic scattering, generally. Earlier measurements have either relied on scattering surface techniques or have depended for their interpretation on a number of assumptions.[1–8] The only existing critical scattering experiment on nickel,[8] in particular, is questionable since but a fraction of the total critical scattering could have been observed.

Many of the over-all features of the long-wavelength low-frequency scattering at the temperature extremes $T\gg T_c$ and $T=0°K$ are now becoming apparent. What is not understood, however, is how the scattering changes in the neighborhood of the critical temperature. In this paper, we seek to present extensive measurements on the scattering in this temperature range. These measurements can be compared and contrasted with recent experiments on the simple antiferromagnet $RbMnF_3$[9] and with our own recent investigations of iron.[10] In general, this earlier work fitted in remarkably well with the theory of critical phenomena, particularly with the predictions derived by Halperin and Hohenberg[11] from the dynamic scaling laws. Three features of the data, however, appeared to raise interesting new questions that require further investigation both experimentally and theoretically. These are (i) below T_c the antiferromagnet shows a scattering spectrum with three peaks; two of these are due to spin waves and the third is believed to arise from diffusive fluctuations in the z component of the spin. The ferromagnet iron showed only the two spin-wave peaks and not the third peak. (ii) The line shape at T_c in iron indicates that there is some sort of a heavily-damped propagative component of the spin fluctuations. (iii) The critical exponent of the spin-diffusion constant in iron was considerably less than is predicted theoretically.

These three points provided extra motivation for carrying out the extensive experimental program necessary to produce the comprehensive data given in the present work.

In Sec. II, we describe briefly the experimental technique, and Sec. III gives the detailed experimental results. This section falls naturally into three parts

* Work performed under the auspices of the U. S. Atomic Energy Commission.
† On leave at Faculty of Science, Osaka University, Osaka, Japan.
‡ On leave from A. E. R. E. Harwell, England; now returned.
§ On leave at State University of New York at Stony Brook.
[1] L. Passell, K. Blinowski, T. Brun, and P. Nielsen, Phys. Rev. **139**, A1866 (1965).
[2] B. Jacrot, J. Konstantinovic, and G. Parette, *Inelastic Scattering of Neutrons and Solids* (International Atomic Energy Agency, Vienna, 1963), p. 317.
[3] G. Shirane, R. Nathans, O. Steinsvoll, H. A. Alperin, and S. J. Pickart, Phys. Rev. Letters **15**, 146 (1965).
[4] S. J. Pickart, H. A. Alperin, V. J. Minkiewicz, R. Nathans, G. Shirane, and O. Steinsvoll, Phys. Rev. **156**, 623 (1967).
[5] S. Spooner and B. L. Averbach, Phys. Rev. **142**, 291 (1966).
[6] D. Bally, B. Garbcev, A. M. Lungu, P. Papovici, and M. Totici, J. Phys. Chem. Solids **28**, 1947 (1967).
[7] M. W. Stringfellow, J. Phys. C **1**, 950 (1968).
[8] D. Cribier, B. Jacrot, and G. Parette, J. Phys. Soc. Japan Suppl. **17**, 67 (1962).
[9] R. Nathans, F. Menzinger, and S. J. Pickart, J. Appl. Phys. **39**, 1237 (1968).
[10] M. F. Collins, V. J. Minkiewicz, R. Nathans, L. Passell, and G. Shirane, Phys. Rev. **179**, 417 (1969); M. F. Collins, R. Nathans, L. Passell, and G. Shirane, Phys. Rev. Letters **21**, 99 (1968).
[11] B. I. Halperin and P. Hohenberg, Phys. Rev. Letters **19**, 700 (1967); and private communication.

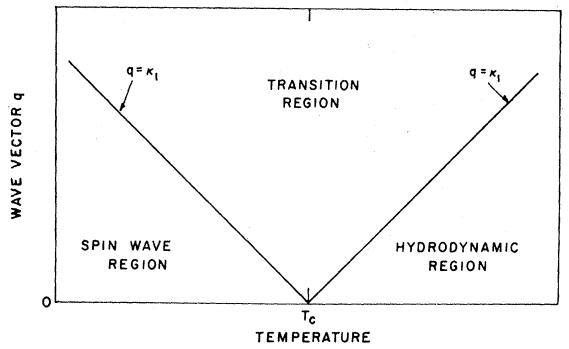

FIG. 1. The figure schematically illustrates the three regions in q-T space for which the behavior of the scattering is different. The lines $q=\kappa_1$ have arbitrarily been taken as the boundaries between the regions. The figure shows that the spin-wave and the hydrodynamic regions become vanishingly small for $T\sim T_c$.

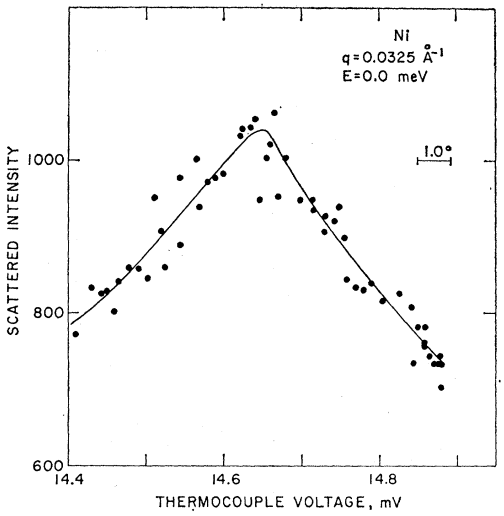

FIG. 2. The figure shows the intensity at $q=0.0325$ Å^{-1} and $\omega=0.0$, as the temperature drifts through T_c. These data serve as the calibration of the thermocouple imbedded in the bottom of the nickel sample. The error with which the transition temperature was determined is illustrated by the solid line in the figure. The peak in the scattering shifted toward higher temperatures and broadened for the higher q values.

corresponding to the three different regions of critical phenomena, as shown schematically in Fig. 1. The first region, known as the *spin-wave region*, corresponds to $T<T_c$ and $q<\kappa_1$, where κ_1 is the critical-range parameter. The second region with $q>\kappa_1$ is the *transition region* and the third, with $T>T_c$ and $q<\kappa_1$, is the *hydrodynamic region*.

The paper concludes in Sec. IV with an over-all discussion of the implications of the experimental data.

II. PRELIMINARY REMARKS

A. Experimental Procedure

The properties of the resolution function of a three-crystal spectrometer have been treated by Cooper and Nathans,[12] and the application of the theory to low-energy spin-wave and critical scattering has been discussed by us[10] in connection with measurements on iron. We have followed just the same experimental procedures as in the iron measurements and will not repeat a description of them here.

The intensity of the magnetic scattering from nickel is typically a quarter of that from iron. Further, the scattering from nickel is more inelastic in the critical region. The resultant diminished cross sections necessitated the use of a lower instrumental resolution in the present experiment compared with our previous work on iron. As a result, smaller values of q (<0.05 Å^{-1}) became inaccessible. Access to the hydrodynamic region above T_c was accomplished by working at higher values of $(T-T_c)/T$, where the κ_1 values are higher.

B. Crystal and Oven

The single crystal used in the experiment was made from the Ni^{60} isotope by J. Hawkey with the help of J. J. Hurst, F. Merkert, and D. E. Cox. The reasons for using the isotopically enriched crystal were that the isotopic incoherent scattering of natural nickel ($\sigma=4.8$ b) is eliminated, and that the phonon scattering is reduced by approximately a factor of 13. The crystal had a cylindrical shape; the diameter and length were 0.5 and 0.9 in., respectively. The data were taken exclusively in the vicinity of [111] to avoid the problem of the energy cutoff $\hbar\omega_{\max}=2Eq/k$ inherent in critical scattering experiments performed in the forward direction (i.e., $\tau=0$).

The oven contained a cylindrical heating element made from molybdenum mesh, surrounded by three heat shields. A copper cylinder was inserted between the sample and the heater mesh to maintain temperature uniformity across the sample. Two chromel-alumel thermocouples were embedded in the sample. The long-term temperature stability of the sample was approximately ±0.5°K, and the temperature gradient across the sample was typically 0.02°K. T_c was obtained from the measurement of the elastic diffuse scattering at small q values as shown in Fig. 2.

III. EXPERIMENTAL RESULTS

A. Spin-Wave Scattering

The data in this region is divided into two parts: (1) the spin waves observed at room temperture and (2) the low-energy scattering observed in the vicinity of the transition region.

Neutron groups of the high-energy spin waves were taken using a number of different incident neutron energies; Fig. 3, for example, contains typical profiles of two groups, one observed with an incident energy of 110 meV, the other with 75 meV. Most of the data were collected in this manner, and the results are

[12] M. J. Cooper and R. Nathans, Acta Cryst. **23**, 357 (1967).

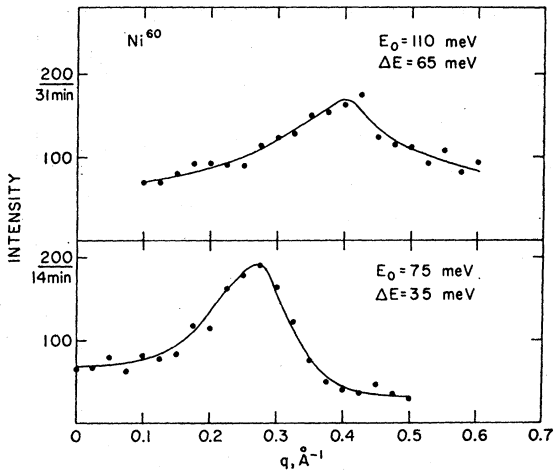

FIG. 3. The neutron groups in the figure are representative of the scattering observed for the high-energy spin waves along [111]. The constant-E mode was used to largely eliminate the error that can be introduced when identifying the peak position as the spin-wave energy.

shown in Fig. 4. We studied the spectrum along two high-symmetry directions, [111] and [110]. A lack of directional anisotropy in the spin-wave energy is readily apparent in the figure. Along the [111], the zone boundary is at 1.54 Å^{-1}, and so the data extend to $q/q_{\max}=0.27$.

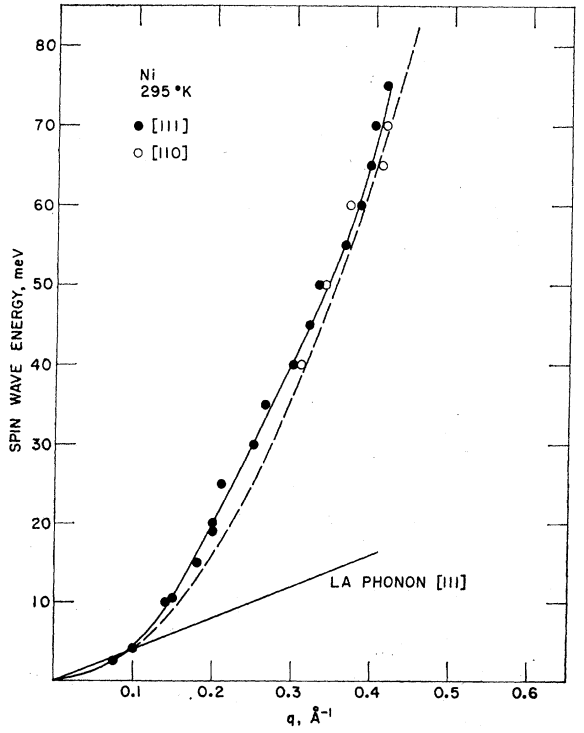

FIG. 4. The spin-wave dispersion relation along [111] and [110]. The dashed curve is a quadratic dispersion with $D=400$ meV Å^2. The figure shows that the coefficient of the quartic term is negative.

The dashed curve in Fig. 4 represents a quadratic dispersion relation $E=Dq^2$, with the stiffness constant $D=400$ meV Å^2. This stiffness constant is consistent with the low-q data and the small-angle scattering experiments of Stringfellow.[7] The most striking feature of the data is that it lies *above* the quadratic-dispersion law, which indicates that the coefficient of the quartic term in the dispersion law is negative. This result is consistent with the observations of Pickart *et al.*[4] who found a quadratic dispersion for nickel when using the diffraction method. Shirane *et al.*,[13] when comparing the results taken by the two techniques, noted that the diffraction method systematically shifted the dispersion relation to lower energies for higher q values, which in the case of nickel, is tantamount to canceling the contribution from the negative quartic term. This same behavior was observed for iron, however, in this case, it had the effect of increasing the already positive value of the quartic-term coefficient. We have attempted to least-squares fit the data to a series expansion in even powers of q and found that the convergence was poor. If such a series expansion is to be useful, then the contribution to the energy from the terms of higher order than q^2 must be small; we found that, in fact, the reverse was generally true for $q>0.25$ Å. Nevertheless, as a means to describe quantitatively the extent of the departure from a simple quadratic dependence, we have estimated the coefficient of the quartic term to be

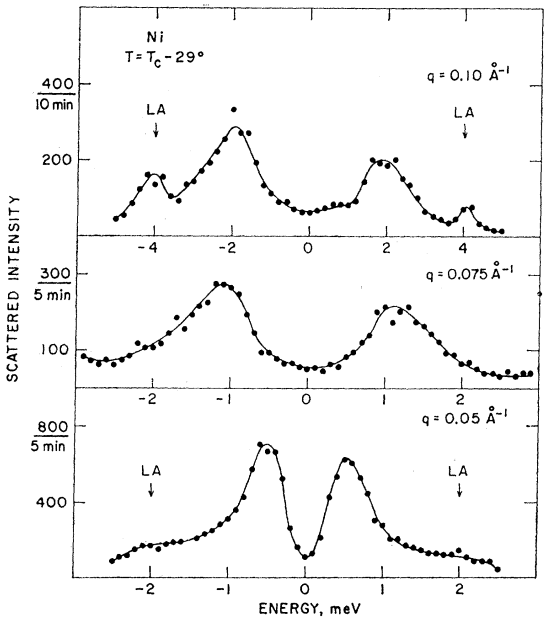

FIG. 5. Typical high-resolution groups that we observe from the low-energy spin waves. The scattering to the left-hand side of the figure is for neutron energy gain; to the right, energy loss. The effect of the resolution of the spectrometer is illustrated by the asymmetric spin-wave groups for $q=0.05$ Å^{-1}. Note that the energy scale has been changed for $q=0.1$ Å^{-1}.

[13] G. Shirane, V. J. Minkiewicz, and R. Nathans, J. Appl. Phys. 39, 383 (1968).

-4200 ± 1500. The solid line in Fig. 4 represents the least-squares fit of the data to an expansion out to q^{10}, and we include it in the figure only as a curve to represent the data.

We now discuss the scattering from the low-energy spin waves, in particular its temperature dependence. Figure 5 contains some representative profiles for $T=T_c-29$°K. The groups in this region were taken in the constant-Q mode of operation because the data could be readily interpreted by the procedure established by Collins *et al.*[10]; for $q=0.05$ Å^{-1}, the effect of the resolution function of the spectrometer, as discussed by them, is clearly reflected in the asymmetric spin-wave line shape. The figure also illustrates that we have not observed a diffusive component in the scattering below T_c. Such a diffusive component in the scattering has been observed[9] in $RbMnF_3$, and its absence in iron and now in nickel is one of the more perplexing aspects of the data.

Since the wave vectors involved are small, a dispersion relation of the form Dq^2 was used to fit the data at each temperature. The temperature variation of the exchange stiffness constant is shown in Fig. 6, where for comparison we have also included the dashed curve to represent the data of Collins *et al.*[10] for iron. We fit the data to the power law $D_0(1-T/T_c)^r$ and find that the power r is 0.39 ± 0.04 and D_0 is 620 ± 100 meV Å^2. Halperin and Hohenberg,[11] from the scaling laws, predict that D will go approximately as $(1-T/T_c)^{1/3}$. Stringfellow,[7] using the small-angle scattering technique, found that D decreases smoothly to ~125 meV Å^2 at $T=T_c$. This is in clear disagreement with our data, since we have observed that $D\sim70$ meV Å^2 for $(1-T/T_c)\sim0.004$. It is most probable that the applied field of 1800 Oe that is used in the small-angle scattering experiment is having a pronounced effect on the spin-wave energy. Similar effects were noted for iron.[10]

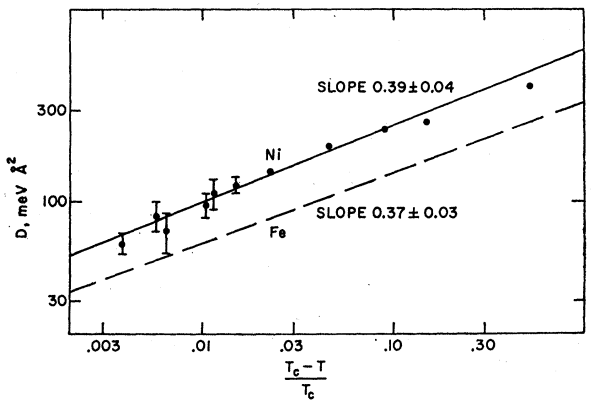

FIG. 6. The temperature variation of the exchange stiffness constant D. The dashed curve represents the data taken by Collins *et al.* for iron. The data seem to indicate that D is scaling as the magnetization. The data are given on a log-log plot; the fit to the straight line would indicate that $D\to0$ as $T\to T_c$.

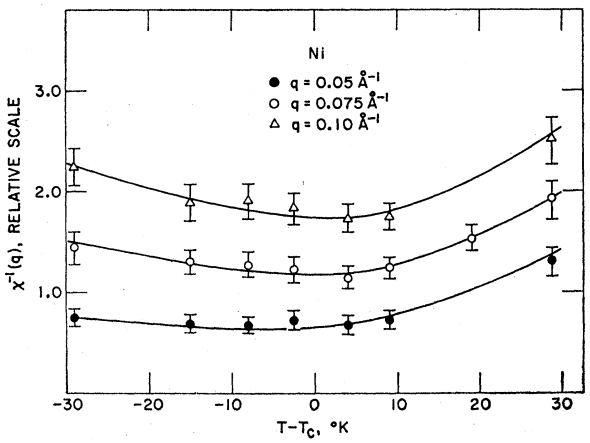

FIG. 7. The temperature variation of the inverse of the static susceptibility through the transition. The data clearly illustrate the need for the kinematic term $\langle S^z\rangle$ in the cross section by the absence of a sharp minimum at $T=T_c$.

Whether D actually goes to zero at T_c is impossible to determine. We observe that the spin waves for $q<0.125$ become over-critically damped just below T_c so that at higher temperatures than this, extraction of meaningful values of D becomes impossible.

Marshall and Murray[14] have shown that kinematic effects can have a great influence on the transverse susceptibility below T_c. Stringfellow[7] has observed this effect in iron and nickel. Assuming for simplicity that spin-wave damping is small, the integrated intensity I varies as[14] $T\langle S^z\rangle/(Dq^2)$. Figure 7 shows that the susceptibility is only very weakly dependent on temperature near T_c at finite q. This is just the sort of behavior to be expected from Marshall and Mruray's equation for the susceptibility, since D and $\langle S^z\rangle$ both tend to zero at T_c according to approximately the same power law.

B. Transition Region

The typical behavior of the scattering that we observe in the transition region is shown in Fig. 8. The *over-all* widths of the distributions are given on the left-hand side of the figure. The diffusive or the Lorentzian distribution that is observed in the hydrodynamic region above T_c anticipates the spin-wave excitations for $T<T_c$ by broadening and "rounding off" the top of the scattering.[15] Again, we note that even at $T_c-4.1$°K, we see no evidence for a third peak in the spectrum. That there is no sudden appearance of an additional scattering near T_c is made evident by the temperature variation of the susceptibility given in Fig. 7. The scattering changes smoothly from one region to the next for finite q. It is interesting to note that if the over-all width of the distributions above T_c are compared with the width of a *single* spin-wave side

[14] W. Marshall and G. Murray, J. Appl. Phys. **39**, 380 (1968).
[15] K. Tomita and T. Kawasaki, J. Phys. Soc. Japan Suppl. **26**, 157 (1968).

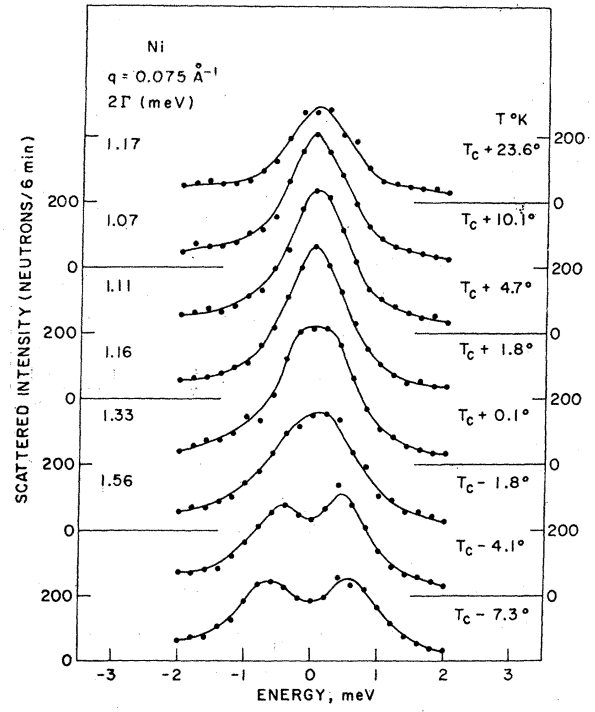

FIG. 8. The figure illustrates typical high-resolution distributions that we observe as the temperature changes from $T<T_c$ to $T>T_c$. The data were collected for $q=0.075$ Å^{-1}. A "rounding off" of the distribution at $T=T_c$ is apparent. The over-all linewidth is given by the column on the left.

band below T_c, they are approximately equal. In other words, the relaxation rate of the fluctuations or the "inelasticity," in addition to the susceptibility $\chi(q)$, varies continuously through T_c for $q\neq 0$. The change of the susceptibility and the linewidth through T_c are strongly wave-vector-dependent; we have observed that the smaller the wave vector, the more rapidly the quantities vary through the ordering temperature.

There are other aspects of the scattering in the transition region that we now discuss, and about which we can be somewhat more quantitative: (1) the over-all linewidth of the distributions and (2) the intensity of the scattering as a function of q. It has been predicted originally by Halperin and Hohenberg,[11] using dynamic scaling theory, that at T_c, $\Gamma \propto q^{5/2-\eta/2}$. In Fig. 9, we plot the half-width of the distributions at half-maximum as a function of the wave vector; the data were collected at T_c, and has been corrected for resolution effects. The resolution corrections for the smaller values of q are, of course, large. For example, the observed width for $q=0.05$ Å was 0.33 meV, and the resolution corrected with is 0.2 meV. The dashed line in the figure represents the data of Collins *et al.*[10] for iron. We find that the exponent is 2.46 ± 0.25 and is in excellent agreement with what had been predicted.

With reference to the q dependence of the static susceptibility, our results give $\chi(q) \propto q^{-1.9\pm0.2}$. The size of the uncertainty precludes our determining Fisher's parameter η but it does allow us to rule out the $q^{-3/2}$ dependence for $\chi(q)$ suggested by Izuyama.[16]

Figure 10 shows the line shape in both iron and nickel at $T=T_c$, plotted after the data has been resolution corrected. Data from a number of different wave vectors q have been superposed assumed that frequencies scale as $q^{5/2}$. The same solid line has been drawn through the data points for iron and nickel except that the frequency scale has been altered by a factor of 2.

C. Hydrodynamic Region

In this region, the spin fluctuations are governed by diffusion processes, and the cross section is given by

$$S(q,\omega)=\frac{2}{3\pi}\frac{S(S+1)}{r_1^2}\frac{1}{\kappa_1^2+q^2}\frac{\Gamma}{\Gamma^2+\omega^2}, \qquad (1)$$

with $\Gamma=\Lambda q^2$, where Λ is the diffusion constant, and κ_1 and r_1 represent, respectively, the range and strength of the spin correlations. In the present experiment, the range of q that was used in the analysis at a given temperature was restricted so that the above equation gave an adequate representation of the data in the least-squares sense. The analysis proceeded in the same manner as was used by Collins *et al.*[10] The differential cross section was convoluted with the resolution function of the spectrometer by computer calculation, and the three parameters, the scaling factor (essentially $1/r_1^2$), the inverse range κ_1, and the diffusion constant were obtained by a least-squares fit to the data at each temperature. Overall, the quality of the fits was satisfactory. The F value, the statistical measure of the

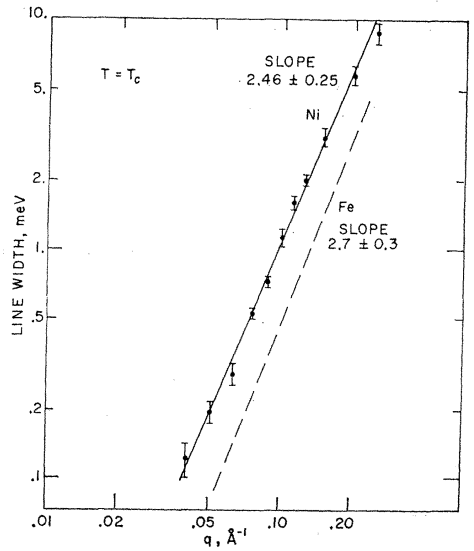

FIG. 9. The figure shows the half-width of the scattering at half-height as a function of wave vector on a log-log plot. The dashed line represents the data of Collins *et al.* for iron. The data agree with the dynamic scaling-law prediction $\Gamma \propto q^{5/2}$.

[16] T. Izuyama, J. Phys. Soc. Japan Suppl. **26**, 109 (1968).

quality of fit, was on the average 1.5 (the corresponding value for iron was 1.2); the *total* range of F was from 0.5 to 2.35. The F values of 1.0 and 1.8 correspond to as good a fit as can be expected from statistical fluctuations alone, and to a statistical error of two standard deviations, respectively. Figure 11 shows the data from one of the poorer statistical fits ($F=2.3$) with the solid line giving the least-squares-fitted intensities from convoluting the resolution function with the cross section of Eq. (1). It is difficult to discern any systematic departures of the data from the expected cross section; any lack of goodness of fit appears to be due to random "noise" in the individual data points.

The boundary between the hydrodynamic and the transition regions, as was evidenced in iron by an abrupt increase in F as the q range was increased to higher values, is not as pronounced in nickel. This breakdown in the form of the cross section given above at the higher q values is directly related to the "rounding off" of the distributions in the transition region; see, for example, the profile in Fig. 8 for $T=T_c$. We conclude that if there is a propagating component in the fluctuation spectrum of nickel above T_c, its relative contribution to the scattering is less than in iron. It is possible that for nickel, the q range for this region can

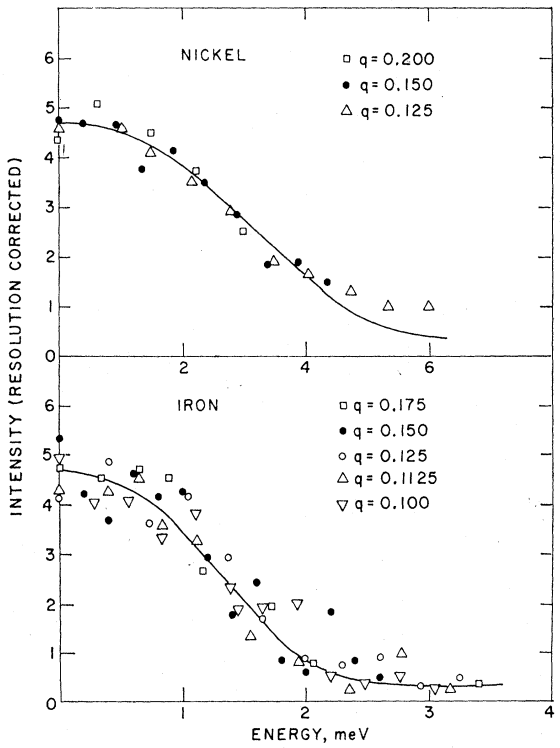

FIG. 10. Resolution-corrected line shapes at T_c for nickel and for iron. The data at different wave vectors have all been scaled to a wave vector of 0.15 Å^{-1} using the dynamic scaling laws. The same solid line has been drawn through the nickel and the iron data with the exception that the frequency scale has been changed by a factor of 2.

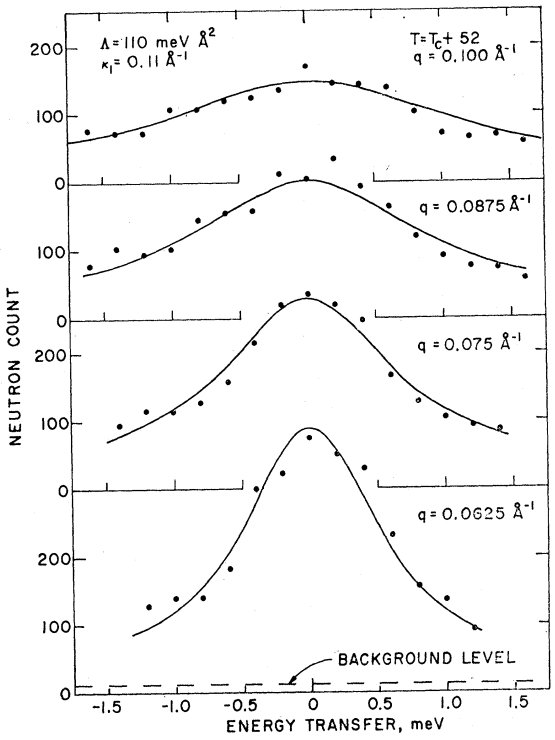

FIG. 11. Scattering in the hydrodynamic region at $T_c+52°$. The solid line is the scattering predicted on the basis of the diffusion equations.

be extended by including terms in q^4 in the relaxation rate Γ and in the denominator of the static term. We did not use this approach because it would extend the number of parameters in the least-squares procedure beyond the point justified by the statistical accuracy of the data.

The quantities that can be established with some certainty are the static susceptibility $\chi(0)$ and the diffusion constant Λ.

The temperature variation of $\chi(0)$ is given in Fig. 12. The most striking feature of the data is that it suggests that the susceptibility is falling off faster then $(1-T_c/T)^{-\gamma}$, with $\gamma=1.34\pm0.01$, the power law that has been established by Kouvel, Kouvel, and Comly.[17] We do not feel that this effect is spurious, since neutron scattering should give reliable information about the exponent γ. In fact, the origin of this apparent contradiction is not hard to find. In deriving a susceptibility we have assumed that the Lorentzian cross section of Eq. (1) is valid at all frequencies. The work of a group at Harwell has shown that there is additional temperature-independent magnetic scattering at high frequencies. The existence of this magnetic scattering can qualitatively account for this apparent increase in γ as observed in this experiment. The effect of not in-

[17] J. S. Kouvel, J. B. Kouvel, and J. B. Comly, Phys. Rev. Letters **20**, 1237 (1968); see also J. E. Noakes and A. Arrott, J. Appl. Phys. **39**, 1235 (1968).

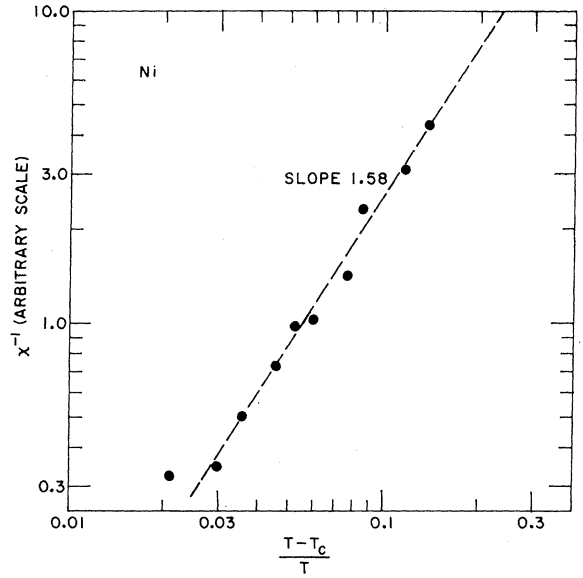

FIG. 12. The figure shows the temperature variation of the static susceptibility $\chi(0)$ as determined in this low-energy scattering experiment. The line with the slope 1.58 represents the data for this temperature interval. The increase in the exponent γ from the $\frac{4}{3}$ power law is a result of not observing all of the scattering at low energy. High-energy scattering that to a large extent is temperature-independent has been observed for nickel by the Harwell group.

cluding the high-energy scattering becomes more pronounced as the temperature is increased since for temperatures close to T_c, the critical scattering dominates the susceptibility, but as the temperature is increased, the intensity of the critical scattering decreases and the relative contribution of the high-energy scattering becomes increasingly more important.

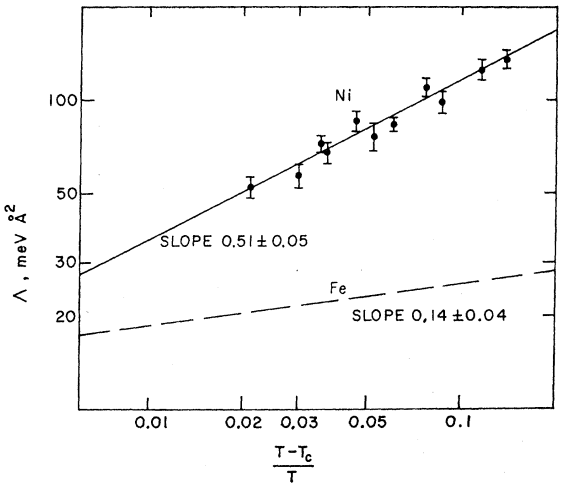

FIG. 13. The temperature variation of the diffusion constant Λ. The dashed line represents the data of Collins *et al.* for iron. It appears that the diffusion process in nickel and in iron is different. The data are given on a log-log plot, and the fit to the straight line indicates that $\Lambda \to 0$ as $T \to T_c$. To obtain the dimensionless parameter $2m\Lambda/\hbar$, multiply the value of Λ 0.483.

The temperature dependence of the diffusion constant Λ is given in Fig. 13; the dashed curve represents the results of Collins *et al.*[10] for iron. It appears from the data that the spin diffusion process in nickel and in iron is different. If we fit the data to the power law $\Lambda_0(1-T_c/T)^P$, the exponent P is 0.51 ± 0.05 and Λ_0 is 380 ± 70 meV Å^2. Kawasaki,[18] and Halperin and Hohenberg[11] have predicted that Λ should vary approximately as $\chi^{-1/4}$. With the exponent for the susceptibility taken from Kouvel, Kouvel, and Comly,[17] the critical exponent for Λ should be approximately 0.33. There is a clear disagreement with experiment. It was not possible to study the relaxation rate in the immediate vicinity above the transition temperature because the hydrodynamic region is too severely restricted in extent.

IV. DISCUSSION AND CONCLUSIONS

A. Spin Waves

If the spin-wave dispersion relation at room temperature is interpreted in terms of a Heisenberg Hamiltonian then, following the general lines of an argument first propounded by Marshall,[19] we conclude that

$$\sum_R J_R \text{ is positive}, \tag{2.1}$$

$$\sum_R J_R R^2 = 4000\pm250 \text{ meV Å}^2, \tag{2.2}$$

$$\sum_R J_R R^4 = -10\,000\,000 \text{ meV Å}^4, \tag{2.3}$$

$$\sum_R J_R R^6 \text{ is negative}, \tag{2.4}$$

where J_R is the exchange interaction between spins that are a distance R apart.

Equation (2.1) is a necessary (but not sufficient) condition for ferromagnetism. In deriving a numerical value for the right-hand side of Eq. (2.3), spherical symmetry has been assumed; this is not correct, but, since the interaction is observed to be long range and without directional anisotropy, it probably gives a reasonable estimate of the quantity involved.

The data implies that the exchange constant J_R must change sign at least once as a function of R. The main contribution from the near neighbors must be ferromagnetic, while antiferromagnetic exchange dominates for more distant neighbors.

B. Critical Exponents

Table I shows the observed critical exponents for various properties of nickel and the exponents predicted on the basis of the scaling laws.[11] For complete-

[18] K. Kawasaki, J. Phys. Chem. Solids 28, 1277 (1967).

[19] W. Marshall, in *Proceedings of the Eighth International Conference on Low-Temperature Physics, London, 1962*, edited by R. O. Davies (Butterworths Scientific Publications Ltd., London, 1963).

TABLE I. Critical exponents in nickel and iron. ν and ν' express the temperature dependence of the inverse range parameter above and below T_c, β the temperature dependence of the magnetization below T_c, γ the temperature dependence of the static susceptibility above T_c, and η the deviation of the scattering in the hydrodynamic region above T_c from the ideal O-Z form.

Property observed	Scaling laws	Exponent Heisenberg (approx.)	Nickel (this paper)	Iron[a]
Linewidth at T_c	$5/2-\eta/2$	2.46	2.46 ± 0.25	$2.7\ \pm0.3$
Spin-wave stiffness	$\nu'-\beta$	0.33	0.39 ± 0.04	0.37 ± 0.03
Diffusion constant	$(\nu/\nu')(\nu'-\beta)$	0.33	0.51 ± 0.05	0.14 ± 0.04
Susceptibility $T>T_c$	γ	1.38	1.58 ± 0.15	1.30 ± 0.06

[a] Reference 10.

ness, we have also included in the table the results of our recent measurements of critical exponents in iron.[10]

The scaling of the linewidths at T_c as q to the power $\frac{5}{2}$ as shown in Figs. 9 and 10 is a notable success for the theory, since the prediction was made in advance of the experimental data. This power law has been the subject of a number of recent theoretical investigations[11,14,20–22] which are all in substantial agreement to within additive factors of $\frac{1}{2}\eta$ (or order 0.04) for the exponents, where η expresses the departure of the scattering in the hydrodynamic region from the ideal Ornstem-Zernicke (O-Z) form. It is remarkable that at $T\gg T_c$ and $T\gg T_c$ the linewidths vary as q^2 for small q while at T_c the variation is $q^{5/2}$.

The spin-wave stiffness constant varies generally in the manner predicted by the scaling laws. However, there seem to be small but significant discrepancies between the observed exponents for nickel and for iron of 0.39 and 0.37, respectively, and the scaling-law prediction of 0.33. This prediction is based on the assumption that $\gamma=1.38$ and $\eta=0.08$. The experimental power law is significantly greater than 0.33. We note that the magnetization scales with exponent β which is observed[17] to be 0.378 ± 0.004 for nickel and is predicted to be 0.39 for a Heisenberg system. Thus, the spin-wave stiffness appears to be scaling according to the same power law as the magnetization, as noted earlier.

It is difficult, and probably impossible, to fit the experimental data above T_c into the framework of existing theories of critical phenomena. The exponent for the diffusion constant in nickel is much larger than would be predicted while that in iron is much lower. One might expect physically that if these materials were to depart from the theoretical predictions they would at least both depart in the same direction. We can only suggest that the anomalous behavior arises from contributions to the spin diffusion from another mechanism over and above that arising from Heisenberg exchange interactions. It is tempting to speculate that this mechanism is a result of the metallic nature of iron and nickel.

The large observed value of γ for nickel can be understood in terms of high-frequency components in the susceptibility[23] that we have not observed. Such effects were not apparent in the iron data[10] because the measurements were confined more closely to the neighborhood of T_c where the contribution of the low-frequency components more effectively dominates the susceptibility. It is noteworthy that the consensus of experimental data for iron and nickel indicates that γ is close to 1.33 in both cases, and certainly less than predicted on the basis of some investigations of high-temperature expansions of the Heisenberg Hamiltonian.[24]

C. Comparison between Spin Dynamics of Iron and Nickel

Here we make a brief comparison between the spin dynamics of nickel as given in this paper and the spin dynamics of iron,[10] the only other ferromagnet for which detailed data are available.

The most readily apparent feature is the qualitative similarity of the spin dynamics of the two materials. In particular, the scattering near to the critical temperature has the same characteristics and no diffusive mode has been observed below T_c. The following general points of contrast are, however, noteworthy: (i) There is no evidence that the exchange interaction in iron changes sign with increasing distance, while this is clearly the case in nickel. (ii) The exponent of the temperature variation of the diffusion constant in nickel and iron are very different (0.51 and 0.14, respectively). This is not understood.

ACKNOWLEDGMENTS

The authors acknowledge the help of J. Skalyo, Jr., in analyzing the data and M. Blume and P. C. Martin in the discussion of our results.

[20] H. Mori and H. Okamoto, J. Phys. Soc. Japan Suppl. **26**, 141 (1968).
[21] P. Résibois, J. Phys. Soc. Japan Suppl. **26**, 127 (1968).
[22] F. Wegner, Z. Physik (to be published).
[23] R. D. Lowde and C. G. Windsor, J. Appl. Phys. **39**, 449 (1968); Solid State Commun. **6**, 189 (1968).
[24] G. A. Baker, H. E. Gilbert, J. Eve, and G. S. Rushbrooke, Phys. Rev. **164**, 800 (1967).